Mon. Not. R. Astron. Soc. **000**, 1–4 (2015) Printed 25 December 2015 (MN LATEX style file v2.2)

Apparent [O III] variability in the narrow line Seyfert I Mrk142

Xue-Guang Zhang⋆ & Long-Long Feng
Institute of Astronomy and Space Science, Sun Yat-Sen University, No. 135, Xingang Xi Road, Guangzhou, 510275, P. R. China

arXiv:1512.07673v1 [astro-ph.GA] 24 Dec 2015

ABSTRACT

In this letter, we checked spectral properties of the well-known narrow line Seyfert I Mrk142, in order to try to find effects of narrow line variability on BLR radius of Mrk142 which is an outlier in the R-L plane. Although, no improvement can be found on BLR radius, apparent narrow line variability can be confirmed in Mrk142. Using the public spectra collected from the Lick AGN Monitoring Project, the spectral scaling method based on assumption of constant [O III] line is firstly checked by examining broad and narrow emission line properties. We find that with the application of the spectral scaling method, there is a strong correlation between the [O III] line flux and the [O III] line width, but weaker correlations between the broad Hα flux and the broad Hβ flux, and between the broad Hα flux and the continuum emission at 5100Å. The results indicate that the assumption of constant [O III] line is not preferred, and caution should be exercised when applying the spectral scaling calibration method. And then, we can find a strong correlation between the [O III] line flux and the continuum emission at 5100Å, which indicates apparent short-term variability of the [O III] line in Mrk142 over about two months.

Key words: Galaxies:Active – Galaxies:nuclei – Galaxies:Seyfert – quasars:Emission lines

1 INTRODUCTION

Emission line variability is a powerful tool to study structures of central emission line regions of active galactic nuclei (AGN). Broad emission line variability has been studied to determine structures of central broad emission line regions (BLR) through the well-known reverberation mapping technique (Blandford & Mckee 1982, Peterson et al. 1993, Bentz et al. 2010, Zhang 2011, Grier et al. 2013, Zhang 2013, Pancoast et al. 2014, Zhang 2015). However, similar methods on narrow line variability is hard to apply to study central narrow emission line regions (NLR) of AGN, because we do not see expected short-term narrow line variability of AGN. Furthermore, when we study broad line variability of AGN, the assumption of a constant narrow line (commonly the [O III] line) is commonly accepted to do the spectral scaling algorithm (Van Groningen & Wanders 1992) to normalize flux calibration of the spectra to a consistent scale for spectra observed with different configurations in different observatories (Peterson et al. 1998, Bentz et al. 2009, and also see references for the other mapped AGN).

However, some results have been reported on narrow line variability. Zheng et al. (1995) reported ten-year narrow line variability in 3c390.3. And, Peterson et al (2013) reported properties of long-term narrow line variability in NGC5548. If there was true short-term narrow line variability (for example, narrow lines from emission regions with high electron density around $10^6 cm^{-3}$, Peterson et al. 2013), the commonly applied spectral scaling calibration method based on constant [O III] line should lead to some unreasonable results. Here, in this letter, based on collected spectra with and without applications of the spectral scaling calibration method, we carefully checked spectral properties of the well-studied mapped AGN Mrk142, and found that the spectral scaling calibration method could be unreasonable, and then report more interesting results on narrow line variability. This letter is organized as follows. Section 2 shows our main results and necessary discussions, and then Section 3 gives our conclusions.

2 MAIN RESULTS

Mrk142 is a well-studied mapped AGN in the Lick AGN monitoring Project (LAMP, http://www.physics.uci.edu/~barth/lamp.html). The main reason to select Mrk142 as the target of this letter is that Mrk142 is the unique outlier in the Radius-Luminosity (R-L) plane for the mapped nearby broad line AGN (Bentz et al. 2013).

⋆ zhangxg23@sysu.edu.cn

© 2015 RAS

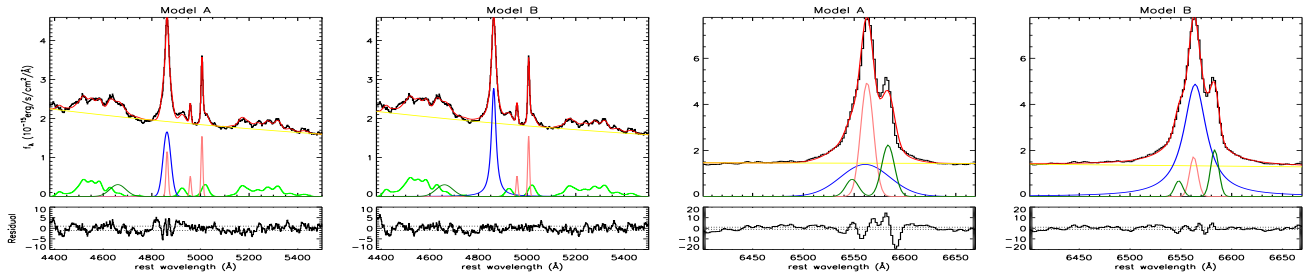

Figure 1. Examples of the best fitted results for emission lines in the final spectrum observed in 12th, April 2008, by different model functions. The left two panels and the right two panels show the results based on Model A and Model B functions for the emission lines around Hβ and around Hα respectively. Top and bottom panels show the best fitted results and the corresponding residuals respectively. In each top panel, solid lines in black, in red, in yellow and in blue show the spectrum, the best fitted results, the power law AGN continuum emission and the determined broad balmer lines respectively. And in the left two top panels, solid lines in green, in dark green and in pink show the Fe II components, the He II line and the narrow Hβ and the [O III] doublet respectively. In the right two top panels, solid lines in dark green and in pink show the [N II] doublet and the narrow Hα respectively. In each bottom panel, the horizontal dotted lines are for $residual = \pm 1$.

Here, we collect the two kinds of spectra of Mrk142 from the LAMP data release: the final reduced spectra (hereafter, 'final spectra') and the scaled spectra after the application of the spectral scaling method (hereafter, 'scaled spectra'). The 'final spectra' are the directly reduced spectroscopic data with flux calibrations determined from nightly spectra of standard stars (typically Feige 34 and BD+284211), which have been well done by the LAMP (more detailed descriptions on the spectroscopic technique can be found in Bentz et al. 2009). Under the assumption of a constant [O III] line, the 'scaled spectra' are obtained by applying the spectral scaling method to the 'final spectra', in order to mitigate the effects of different observational configurations. Then, we can carefully check the emission lines in the spectra of Mrk142.

Before proceeding further, there are three points we should note. First and foremost, as discussed in Park et al. (2012) and Hu et al. (2015), an additional star component could be included in the spectra of Mrk142. However, when we try to add a star component to describe the LAMP spectrum of Mrk142, it is hard to find a clear and stable star component. And moreover, even without a star component, the best description of the emission lines can be achieved. Therefore, we do not consider an additional star component in this letter any more. Different model functions can be applied to describe emission lines, such as gaussian functions, lorentz functions, gauss-hermite functions, etc.. Actually, for the emission lines of Mrk142, simple gaussian or lorentz functions are good enough to describe them, which can be assured by the results shown in the following Figure 1. Therefore, we do not discuss more complex model functions for the emission lines. Last but not least, we should note that there are apparent effects of slit losses, variable seeing and transparency etc. on the measured line parameters from the final spectra. In order to mitigate the effects, the spectral scaling method is commonly applied. Therefore, if the spectral scaling method was preferred, we would expect stronger parameter correlations from the scaled spectra than from the final spectra, because problems with the final spectra have been corrected as much as possible. Hence, we mainly focus on the comparisons between the results from the final spectra and from the scaled spectra.

Now, the emission lines can be described as follows for the emission lines around Hβ (Fe II, He II, Hβ and [O III] doublet) and around Hα (Hα and [N II] doublet). The Fe II template in Kovacevic et al. (2010) is applied to describe the optical Fe II lines, a power law function is applied to describe the AGN continuum emission, a broad gaussian function is applied to describe the He II line, two narrow gaussian functions are applied to describe the [O III] (the [N II]) doublet. And, when the [O III] and [N II] doublets are described by the gaussian functions, their flux ratios are fixed to the theoretical values ($f_{5007}/f_{4959} = f_{6585}/f_{6549} = 3$). For the broad and narrow balmer lines, two different model functions applied, Model A: one broad plus one narrow gaussian functions, Model B: one broad lorentz function plus one narrow gaussian function. For the model functions applied to the narrow balmer lines, they have the same line widths. Here, a very weak narrow He II line is not considered. Then, through the Levenberg-Marquardt least-squares minimization technique, the emission lines can be well fitted.

Figure 1 shows examples of the best fitted results for the emission lines by the model functions. We can clearly see that the lorentz functions for the broad balmer lines can lead to better fitted results, due to smaller residuals around Hβ and Hα. Here, the residuals are calculated by $\frac{y_{obs}-y_{fit}}{y_{err}}$, where y_{obs}, y_{err} and y_{fit} represent the observed values, the corresponding uncertainties and the best fitted results respectively. Therefore, in this letter, only Model B is considered, and no complex model functions are discussed. Then, we carefully check the line parameters determined from Model B as follows.

First and foremost, we checked line parameter correlations of the [O III] line. If the spectral scaling method was preferred, we would expect no line parameter correlation to be found for the [O III] lines in the scaled spectra of Mrk142. Figure 2 shows the correlations between line flux and line width of the [O III] lines in the scaled spectra and in the final spectra respectively. In the scaled spectra, there is a apparent linear correlation with spearman rank correlation coefficient about 0.49 with $P_{null} \sim 10^{-4}$. But, there is no clear linear correlation from the final spectra. Therefore, by the correlations shown in Figure 2, the applied spectral scaling calibration method is not preferred.

Besides, we checked flux correlations between the broad balmer lines. If the application of the spectral scaling cali-

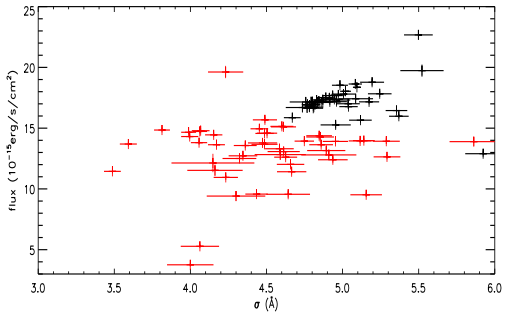

Figure 2. On the correlations between line flux and line width of the [O III] lines in the scaled spectra (symbols in black) and in the final spectra (symbols in red) respectively.

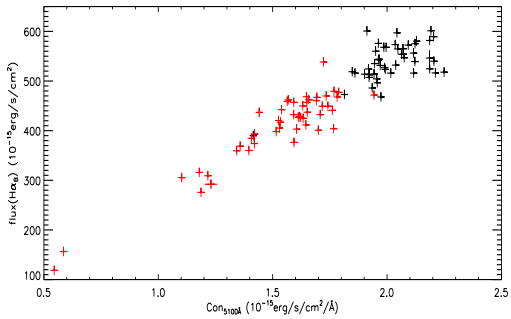

Figure 4. On the correlations between broad line flux of Hα and continuum emission at 5100Å from the scaled spectra (symbols in black) and from the final spectra (symbols in red) respectively.

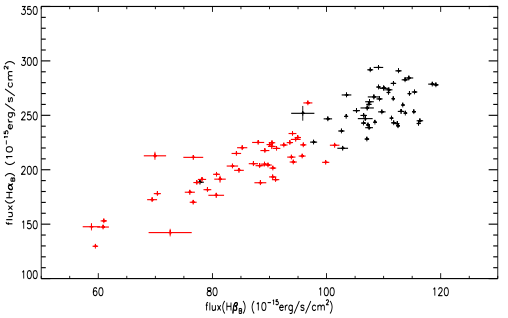

Figure 3. On line flux correlations between the broad balmer lines in the scaled spectra (symbols in black) and in the final spectra (symbols in red) respectively.

bration method were reasonable, a stronger line flux correlation could be expected from the scaled spectra than from the final spectra. Figure 3 shows the broad line flux correlations. The spearman rank correlation coefficients are about 0.44 with $P_{null} \sim 10^{-3}$ and 0.79 with $P_{null} \sim 10^{-11}$ for the broad balmer lines in the scaled spectra and in the final spectra respectively. Therefore, the results in Figure 3 also indicate that the spectral scaling calibration method is not preferred.

Last but not least, we checked the correlations between continuum emission at 5100Å and broad line flux of Hα in the scaled spectra and in the final spectra respectively, which are shown in the Figure 4. Here, similar to what was done by Greene & Ho (2005), the line flux of broad Hα includes the contributions from the [N II] doublet and the narrow Hα. The spearman rank correlation coefficients are about 0.49 with $P_{null} \sim 10^{-4}$ and 0.81 with $P_{null} \sim 10^{-12}$ for the parameters from the scaled spectra and from the final spectra respectively. Therefore, the results shown in Figure 4 also indicate that the spectral scaling calibration method is not preferred, otherwise a stronger linear correlation could be expected from the scaled spectra.

Based on the results above, after careful consideration, we concluded that the assumption of constant [O III] lines to do the spectral scaling calibration is probably not reasonable for Mrk142, which indicates possible [O III] variability to some extent. Then, we can show one rough but interesting check for the [O III] line variability in Mrk142 through the collected final spectra. Certainly, the absolute flux calibration of the final spectra is based on the spectra of standard stars, which tends to give more reliable results on line flux than on line width. However, we should note that it is hard to correct the effects of slit losses, variable seeing and transparency etc. on the line parameters from the final spectra, once we have accepted that the spectral scaling method is not preferred. Therefore, we still show the comparisons on the [O III] line flux to check variability of the [O III] line.

Figure 5 shows the correlation between [O III] line flux and continuum emission at 5100Å(broad Hβ line flux). There are strong linear correlations with spearman rank correlation coefficients of about 0.87 with $P_{null} \sim 10^{-17}$ and 0.93 with $P_{null} \sim 10^{-22}$ for the correlations on continuum emission and on broad Hβ line flux respectively from the final spectra. The strong correlations indicate there is reliable short-term [O III] variability over about two months. Furthermore, we should note that in some final spectra, the measured [O III] line widths are smaller or larger than the mean value (that is another reason why it is necessary to do the spectral scaling calibration). Even the spectra with smaller or larger [O III] line widths are rejected by $|\sigma - \bar{\sigma}| > 0.5$Å, the correlations are still strong with coefficients about 0.89 with $P_{null} \sim 10^{-14}$ and 0.93 with $P_{null} \sim 10^{-18}$ respectively. Furthermore, from the scaled spectra, the linear correlation between [O III] line flux and continuum emission at 5100Å (broad Hβ line flux) can also be found, although there is a small variability amplitude in the [O III] line flux. The spearman rank correlation coefficients are about 0.51 with $P_{null} \sim 10^{-4}$ and 0.48 with $P_{null} \sim 10^{-4}$ for the correlations on continuum emission and on broad Hβ line flux respectively for the parameters from the scaled spectra. It is clear that the results shown in Figure 5 can not be explained by the effects of slit losses, variable seeings and transparency etc., because of no dependence of random slit losses on central continuum emission (broad balmer line emission) and because of such tiny variability of seeings and air masses during the observational period for Mrk142.

Before the end of the subsection, there are three points we should discuss further. First and foremost, we do not consider the effects of probable contributions of star components. Actually, our measured line parameters (especially for the [O III] line) do not depend on whether there are contributions from star components. Therefore, the results above

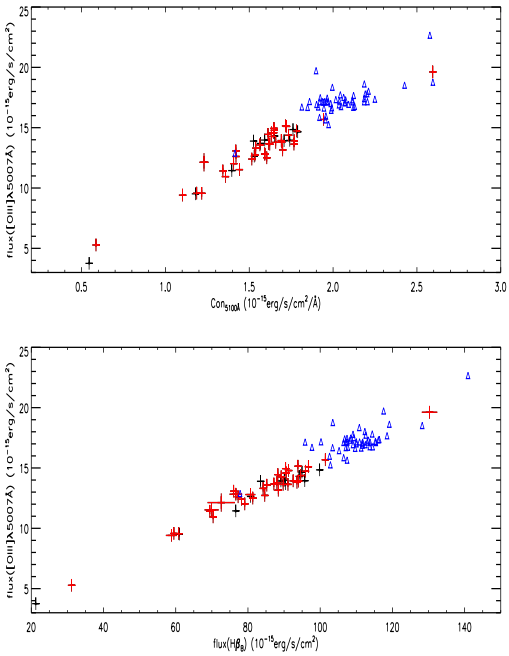

Figure 5. On the correlation between [O III] line flux and continuum emission at 5100Å (top panel), and the correlation between [O III] line flux and broad Hβ line flux (bottom panel), using the final spectra (symbol of plus) and using the scaled spectra (symbol of triangle). In each panel, plus symbols in black represent the values from the final spectra with smaller or larger [O III] line widths.

on the line parameters can be well accepted. Besides, we can be sure that the spectral scaling calibration method is not preferred for the spectral of Mrk142. However, no improved results on BLR radius can be found on cross-correlation of the variability of continuum emission and broad line emission (time lag from the cross-correlation function is still near zero), even with considerations of the [O III] variability. And moreover, due to expected [O III] variability, it is hard to correct the effects of slit losses, variable seeings and transparency etc. on the line parameters from the final spectra. In other words, we can not give a clearer conclusion on the [O III] variability with a reliable variability amplitude, but we can find strong evidence to support the [O III] variability. Last but not least, we also tried to check the spectral properties of several another mapped AGN by the same procedures above, but we can not find similar results as those of Mrk142. In other words, the spectral scaling calibration method with the assumption of a constant [O III] line could be commonly accepted to some extent, but caution should be exercised when applying the calibration method. And checking corresponding correlations on spectral parameters in the spectra with and without the application of a calibration method could provide further information on whether the calibration method is preferred.

3 CONCLUSIONS

Finally, our main conclusions are as follows. On the one hand, we carefully checked whether the spectral scaling calibration method is preferred for the LAMP final spectra of Mrk142, and we can find that with the application of the spectral scaling calibration method based on the assumption of constant [O III] line, we do not find any stronger parameter correlations. Therefore, the commonly applied spectral scaling calibration method, based on the assumption of a constant [O III] line (especially constant [O III] line flux) is not preferred for the spectra of Mrk142. On the other hand, we find there is reliable variability of the [O III] line, based on the strong correlations between [O III] line flux and continuum emission, and between [O III] line flux and broad balmer line flux.

ACKNOWLEDGEMENTS

Zhang and FLL gratefully acknowledge the anonymous referee for giving us constructive comments and suggestions to greatly improve our paper. Zhang acknowledges the kind support from the Chinese grant nsfc-u1431229. FLL is supported under the NSFC grants 11273060, 91230115 and 11333008, and State Key Development Program for Basic Research of China (No. 2013CB834900 and 2015CB857000). This work has made use of data from the Lick AGN Monitoring Project public data release.

REFERENCES

Bentz, M. C., Walsh, J. L., Barth, A., Baliber, N., Bennert V. N., et al., 2009, ApJ, 705, 199
Bentz, M. C., Horne, K., Barth, A., Bennert V. N., Canalizo G., et al., 2010, ApJ, 720, L46
Bentz, M. C., Denney, K. D., Grier, C. J., Barth, A. J., Peterson, B. M., et al., 2013 ,ApJ, 767, 149
Blandford, R. D., & Mckee, C. F., 1982, ApJ, 255, 419
Greene, J. E. & Ho, L. C., 2005, ApJ, 630, 122
Grier, C. J., Peterson, B. M., Horne, K., Bentz, M. C., Pogge, R. W., et al., 2013, ApJ, 764, 47
Hu, C., Du, P., Lu, K. X., Li, Y. R., Wang, F., et al., 2015, ApJ, 804, 138
Kovacevic, J., Popovic, L. C., Dimitrijevic, M. S., 2010, ApJS, 189, 15
Pancoast A., Brewer B. J., Treu T., Park D., Barth A. J., Bentz M. C., Woo J.-H., 2014, MNRAS, 445, 3073
Park, D., Woo, J.-H., Treu, T., Barth, A. J., Bentz, M. C., et al., 2012, ApJ, 747, 30
Peterson, B. M., 1993, PASP, 105, 247
Peterson, B. M., Wanders, I., Bertram, R., Hunley, J. F., Pogge, R. W., Wagner, R. M. 1998, ApJ, 501, 82
Peterson B. M., Denney, K. D., Rosa, G. D., et al., 2013, ApJ, 779, 109
Van Groningen, E & Wanders I., 1992, PASP, 104, 700
Zhang X. G., 2011, MNRAS, 416, 2857
Zhang X. G., 2013, MNRAS Letter, 431, 112
Zhang X. G., 2015, MNRAS Letter, 447, L35
Zheng W., Perez E., Grandi S. A., Penston M. V., 1995, ApJ, 109, 2355

Table 1. Line parameters

HJD	scaled spectra					final spectra				
	con	f_β	f_α	σ_3	f_3	con	f_β	f_α	σ_3	f_3
4550	2.2±0.1	112.3±0.3	242.4±0.9	5.0±0.1	18.1±0.1	1.1±0.1	59.4±0.5	129.6±1.1	4.4±0.1	9.5±0.1
4551	1.9±0.1	102.5±0.5	235.5±1.2	5.3±0.1	15.2±0.1	1.7±0.1	89.1±0.7	205.1±1.4	5.2±0.1	13.1±0.2
4553	2.0±0.1	113.3±0.2	259.4±0.7	4.8±0.1	17.2±0.1	1.7±0.1	95.9±0.5	222.8±1.4	4.0±0.1	14.3±0.1
4555	2.5±0.1	140.9±1.5	325.8±4.3	5.4±0.1	22.1±0.3	1.1±0.1	58.8±1.5	147.6±3.4	4.2±0.1	9.4±0.4
4556	2.1±0.1	111.7±0.4	243.0±1.2	4.8±0.1	17.4±0.1	1.9±0.1	101.4±0.8	222.5±1.9	4.4±0.1	15.±0.2
4557	1.9±0.1	110.9±0.6	273.4±1.2	5.1±0.1	17.3±0.2	1.5±0.1	90.1±0.5	223.1±1.1	5.1±0.1	13.1±0.1
4558	2.1±0.1	118.5±0.7	278.6±1.2	4.9±0.1	17.0±0.2	1.7±0.1	94.6±0.8	227.8±1.3	4.8±0.1	14.0±0.2
4559	1.9±0.1	107.4±0.7	238.6±1.4	5.1±0.1	15.2±0.2	1.7±0.1	95.7±0.6	212.5±1.3	5.1±0.1	13.2±0.2
4560	2.0±0.1	115.4±0.5	271.4±1.1	4.8±0.1	17.2±0.1	1.6±0.1	92.5±0.6	222.7±1.3	4.7±0.1	13.0±0.1
4561	1.9±0.1	105.2±0.6	254.3±1.5	5.3±0.1	16.1±0.2	1.5±0.1	80.7±0.6	195.8±1.4	5.2±0.1	12.1±0.2
4562	2.2±0.1	114.4±0.7	284.3±1.8	5.2±0.1	17.1±0.2	1.1±0.1	60.9±0.5	152.9±1.3	5.1±0.1	9.5±0.1
4564	2.0±0.1	111.6±0.2	265.2±0.8	4.7±0.1	17.2±0.1	1.7±0.1	94.9±0.5	229.6±1.3	3.9±0.1	14.1±0.1
4566	2.1±0.1	113.7±0.6	282.6±0.9	5.0±0.1	16.2±0.1	1.7±0.1	94.0±0.6	233.2±1.1	4.9±0.1	13.2±0.2
4567	2.0±0.1	115.2±0.3	253.2±1.1	4.8±0.1	17.2±0.1	1.6±0.1	89.7±0.6	204.3±1.5	4.1±0.1	13.1±0.1
4568	2.0±0.1	114.5±0.3	269.9±0.9	4.7±0.1	16.2±0.1	1.6±0.1	93.6±0.5	224.9±1.4	4.0±0.1	13.1±0.1
4569	2.0±0.1	116.1±0.3	242.4±0.9	4.8±0.1	17.2±0.1	1.7±0.1	99.8±0.6	206.7±1.5	3.8±0.1	14.1±0.1
4570	1.9±0.1	113.7±0.3	252.0±0.7	4.7±0.1	17.0±0.1	1.6±0.1	94.1±0.6	207.0±1.4	3.9±0.1	14.1±0.1
4572	1.9±0.1	109.6±0.6	253.1±1.3	4.8±0.1	16.2±0.2	1.4±0.1	79.1±0.7	181.6±1.3	4.6±0.1	12.1±0.2
4573	1.9±0.1	112.5±0.3	240.3±1.7	4.8±0.1	16.0±0.1	1.5±0.1	90.4±0.7	221.4±2.4	3.5±0.1	13.3±0.2
4575	1.4±0.1	77.8±0.7	188.5±1.1	5.9±0.1	12.1±0.2	1.5±0.1	83.5±0.9	203.3±1.6	5.8±0.1	13.2±0.3
4581	1.9±0.1	111.3±0.3	247.4±0.9	4.7±0.1	16.1±0.1	1.3±0.1	76.6±0.6	170.1±1.6	3.4±0.1	11.0±0.1
4582	1.9±0.1	107.2±0.3	241.1±0.8	4.8±0.1	17.2±0.1	1.6±0.1	90.5±0.5	201.5±1.2	4.4±0.1	14.1±0.1
4583	1.9±0.1	107.1±0.4	228.1±1.2	4.8±0.1	17.3±0.1	1.6±0.1	90.6±0.6	193.4±1.6	4.5±0.1	14.1±0.2
4584	1.8±0.1	100.2±0.7	246.7±1.5	4.9±0.1	17.1±0.2	0.5±0.1	31.1±0.5	74.4±0.9	4.0±0.1	5.2±0.1
4585	1.8±0.1	97.7±0.6	225.3±1.7	4.8±0.1	16.1±0.2	1.4±0.1	76.0±0.8	179.3±2.1	4.6±0.1	13.2±0.2
4587	1.9±0.1	110.8±0.3	270.9±0.8	5.0±0.1	18.1±0.1	1.6±0.1	90.4±0.5	224.8±1.4	4.4±0.1	14.3±0.1
4588	1.9±0.1	108.4±0.3	243.6±0.7	4.9±0.1	17.3±0.1	1.6±0.1	88.2±0.7	203.7±1.4	4.1±0.1	14.4±0.1
4589	1.8±0.1	103.4±0.3	248.9±0.8	4.7±0.1	16.1±0.1	1.6±0.1	91.2±0.6	219.6±1.4	4.0±0.1	14.1±0.2
4590	1.9±0.1	107.4±0.5	260.1±1.2	4.9±0.1	17.3±0.1	1.4±0.1	77.2±0.6	188.2±1.4	4.6±0.1	12.1±0.1
4591	1.9±0.1	106.5±0.6	249.8±1.4	4.6±0.1	15.1±0.1	1.5±0.1	84.6±0.8	199.4±1.9	4.3±0.1	12.2±0.2
4592	2.0±0.1	112.6±0.5	290.8±0.8	4.9±0.1	17.3±0.1	1.5±0.1	84.2±0.8	214.9±1.2	4.5±0.1	13.1±0.2
4593	2.0±0.1	109.2±0.5	265.0±1.3	4.8±0.1	17.0±0.1	1.3±0.1	69.4±0.8	172.4±1.6	4.6±0.1	11.2±0.2
4594	2.1±0.1	108.2±1.1	266.9±2.1	4.9±0.1	17.5±0.3	1.5±0.1	78.2±0.7	191.0±1.6	4.9±0.1	12.1±0.2
4595	2.5±0.1	103.4±0.8	268.7±1.9	5.1±0.1	18.1±0.2	0.5±0.1	21.2±0.5	56.9±0.8	3.9±0.1	3.7±0.1
4596	2.1±0.1	119.1±0.5	277.9±1.2	5.0±0.1	18.6±0.1	1.6±0.1	87.2±0.8	205.5±1.7	4.4±0.1	13.1±0.2
4597	1.9±0.1	107.5±0.7	262.4±1.4	4.9±0.1	17.2±0.2	1.6±0.1	89.2±0.8	217.6±1.5	4.8±0.1	14.2±0.2
4598	2.1±0.1	107.1±1.2	256.7±2.2	4.7±0.1	16.3±0.3	1.2±0.1	60.8±1.1	147.3±1.6	4.6±0.1	9.5±0.2
4600	2.0±0.1	111.7±0.5	279.3±0.8	4.7±0.1	16.2±0.1	1.6±0.1	88.1±1.1	225.0±1.3	4.4±0.1	13.1±0.2
4601	2.1±0.1	95.8±2.1	251.8±6.7	4.7±0.1	17.3±0.3	1.4±0.1	69.9±1.9	212.7±3.7	4.1±0.1	11.2±0.4
4602	1.9±0.1	106.4±0.5	242.8±0.9	4.8±0.1	17.1±0.1	1.7±0.1	93.8±0.7	211.6±1.5	4.6±0.1	15.3±0.2
4603	2.0±0.1	109.0±0.4	275.9±0.8	4.7±0.1	16.6±0.1	1.3±0.1	70.3±0.6	178.0±1.2	4.2±0.1	10.6±0.1
4604	1.9±0.1	110.1±0.4	275.1±1.1	4.7±0.1	17.8±0.1	1.5±0.1	85.2±0.9	220.2±1.7	4.3±0.1	13.7±0.2
4605	1.9±0.1	107.6±0.5	291.8±0.9	4.7±0.1	16.9±0.1	1.7±0.1	96.7±0.8	261.3±1.4	4.6±0.1	15.3±0.2
4607	2.1±0.1	109.0±0.8	293.9±1.3	5.0±0.1	17.4±0.2	1.5±0.1	76.6±1.7	211.3±2.1	4.5±0.1	12.5±0.4
4608	2.2±0.1	113.0±0.5	253.5±2.1	4.8±0.1	17.9±0.1	1.6±0.1	81.3±1.1	191.3±3.2	4.3±0.1	12.2±0.3
4613	2.1±0.1	106.7±1.3	246.9±1.9	5.0±0.1	17.6±0.3	1.5±0.1	80.6±1.4	176.5±2.3	4.9±0.1	12.4±0.4
4614	1.9±0.1	102.8±0.9	219.7±1.7	4.9±0.1	15.7±0.2	1.6±0.1	88.4±1.1	188.0±1.8	4.8±0.1	13.2±0.3
4615	2.4±0.1	128.2±0.6	316.5±1.4	4.9±0.1	18.1±0.1	2.5±0.1	130.2±2.1	342.6±3.2	4.2±0.1	19.8±0.5
4616	2.2±0.1	116.3±0.6	244.9±1.1	4.9±0.1	17.6±0.1	1.7±0.1	91.1±0.6	190.8±1.2	4.8±0.1	13.2±0.2
4617	1.9±0.1	110.1±0.8	274.8±2.1	5.0±0.1	17.6±0.2	8.8±0.1	482.6±6.1	1230.3±12.3	4.9±0.1	75.9±1.5
4618	1.8±0.1	117.5±2.4		5.5±0.1	19.4±0.5	1.2±0.1	72.6±3.7	142.2±3.5	4.1±0.2	12.3±0.7

Note: the first column shows the HJD information, the Second to the sixth columns show the parameters from the scaled spectra: the continuum emission at 5100Å in unit of $10^{-15}erg/s/cm^2/Å$, the line fluxes of broad Hβ (f_β) and broad Hα (f_α) in unit of $10^{-15}erg/s/cm^2$, the second moment of the [O III] line (σ_3) in unit of Å, and the line flux of [O III] (f_3) in unit of $10^{-15}erg/s/cm^2$. The last five columns shows the parameters from the final spectra.